Pure Appl. Geophys. 173 (2016), 3955–3971

DOI 10.1007/s00024-016-1392-y

Pure and Applied Geophysics

A Pilot Tsunami Inundation Forecast System for Australia

Stewart C. R. Allen[1] and Diana J. M. Greenslade[1]

Abstract—The Joint Australian Tsunami Warning Centre (JATWC) provides a tsunami warning service for Australia. Warnings are currently issued according to a technique that does not include explicit modelling at the coastline, including any potential coastal inundation. This paper investigates the feasibility of developing and implementing tsunami inundation modelling as part of the JATWC warning system. An inundation model was developed for a site in Southeast Australia, on the basis of the availability of bathymetric and topographic data and observations of past tsunamis. The model was forced using data from T2, the operational deep-water tsunami scenario database currently used for generating warnings. The model was evaluated not only for its accuracy but also for its computational speed, particularly with respect to operational applications. Limitations of the proposed forecast processes in the Australian context and areas requiring future improvement are discussed.

1. Introduction

The Joint Australian Tsunami Warning Centre (JATWC) is jointly operated by the Australian Bureau of Meteorology and Geoscience Australia. It provides a comprehensive, independent tsunami warning service to advise the media, public and emergency authorities of any tsunami threat to Australia and its offshore territories. JATWC tsunami warnings are issued according to a technique described in Allen and Greenslade (2010). This technique is based on a database of pre-computed tsunami scenarios (T2; Greenslade et al. 2009; Greenslade et al. 2010). When an earthquake occurs, the closest T2 scenario (based on geographic location and earthquake magnitude) is inspected, and wave amplitudes are scaled if necessary. To be more precise, since only the earthquake epicentre is known in real time, and not the rupture direction, all possible T2 scenarios that incorporate the earthquake location are selected (this could be up to 10 scenarios for a Moment Magnitude (M_W) $\geq$8.8 event, fewer for a lower magnitude event), and the warning is based on the worst case. Warning decisions are based on wave amplitudes of the relevant T2 scenario within coastal zones surrounding Australia and its offshore territories. These zones extend approximately 100 km offshore and can cover stretches of coastline ranging from approximately 60 to 600 km. They were designed for general marine warning purpose, rather than specifically for tsunami warning.

Tsunami warnings from the JATWC for each coastal zone are categorised into several levels of threat, namely:

1. *No threat.*
2. *Marine threat*. Indicating potentially dangerous waves and strong ocean currents in the marine environment.
3. *Land threat*. Indicating major land inundation of low-lying coastal areas, dangerous waves and strong ocean currents.

Threshold amplitude values for each threat level have been derived through analysis of observed impacts for past events. Given that historical records are available for only a short time period and no observations for which a land threat would have been issued for Australia exist, it has been difficult to determine the appropriate threshold for a land threat, and therefore, this is currently set at a relatively conservative value. Uslu and Greenslade (2013) used inundation modelling results from a tsunami hazard assessment study for New South Wales (NSW State Emergency Service and Office of Environment and Heritage 2012) to evaluate the threshold values for the JATWC tsunami warnings. The general

[1] Research and Development Branch, Australian Bureau of Meteorology, GPO Box 1289, Melbourne, VIC 3001, Australia. E-mail: stewart.allen@bom.gov.au

conclusion from that study was that the threshold values were appropriate.

One limitation to the existing JATWC system is that a land threat warning indicates that inundation is expected to occur within a coastal zone, but it does not give any detailed information about the level of inundation, i.e., the maximum run-up, the inundation extent, or any information about the areas within the coastal zone that are more likely to be affected. If a land threat were to be issued for any particular coastal zone, JATWC's recommended action is for people within the coastal zone to go to higher ground at least 10 m above sea level, or move at least 1 km away from the coast. These values have been estimated based on a worst case scenario, and the recommended actions apply to a 'one-size-fits-all' tsunami inundation event. More detailed information on the expected inundation for any particular event would be highly valuable to emergency managers, to reduce unnecessary evacuations. This sort of information, however, can only be achieved through detailed inundation modelling. A further limitation is that the existing T2 scenario database is limited to water depths greater than 20 m, with the warnings carefully calibrated, so that amplitude values in waters deeper than 20 m can serve as a proxy for impacts at the coast. This 20-m depth limitation means that coastal tide gauges, a vital source of information for tsunami warning and verification purposes, are not in the model domain, so cannot be used within the existing system for direct model verification.

Tsunami inundation modelling has been undertaken for numerous tsunami hazard assessment studies (e.g. NSW State Emergency Service and Office of Environment and Heritage 2012; Grilli et al. 2015; Gonzalez et al. 2005) and hindcast studies (e.g. Horspool and Griffin 2010; Borrero et al. 2006; Lovholt et al. 2012; Wei et al. 2015). Indeed, the modelling software ComMIT (Titov et al. 2011) provides the capability for anyone, once trained, to undertake their own inundation modelling. However, there are a few real-time, operational systems that are able to provide inundation forecasts during a tsunami event (Bernard and Titov 2015). One example of a tsunami forecast system incorporating forecasts of tsunami inundation is NOAA's Short-term Inundation Forecast for Tsunamis (SIFT) system (Tang et al. 2009) which became operational at NOAA Tsunami Warning Centres in 2013.

In this paper, we describe the development and testing of a pilot inundation forecast system for Australia, and discuss a number of issues relating to the development of a fully operational tsunami inundation forecast system for Australia.

2. *Operational Protocols*

As mentioned in the previous section, the existing forecast guidance for the JATWC is based on a pre-computed database of deep-water tsunami scenarios. This system was developed after the 2004 Indian Ocean tsunami, at a time when computational power was insufficient to consider running tsunami propagation and/or inundation models dynamically within the short time-frames required for tsunami warning.

Given the continuing advances in computational capacity, it is worthwhile to consider what options might exist now or in the near-future for operational tsunami inundation systems. All systems envisaged would necessarily need to be composed of two steps: first, to obtain appropriate offshore boundary conditions for a coastal inundation model and second, to run an inundation model to determine the inundation extent for the coastal region of interest. Either of these steps may be undertaken dynamically, or may be pre-computed. Here, we briefly describe and discuss a few possible operational protocols.

The most straightforward approach given the existing JATWC operational procedures would be to use the relevant deep-water T2 scenario(s) to identify coastal zones that are under threat or near threat. Within these areas, those T2 scenarios could then be used as boundary conditions for any inundation models located within these zones.

A second option is a slight variation of the first approach, and involves the use of real-time tsunameter observations to select the best T2 scenario from a wide range of options, rather than the worst case of a set of possible T2 scenarios, as is currently undertaken operationally. This best T2 scenario would then be used to provide boundary conditions

for the inundation modelling. This would be similar to NOAA's SIFT system, where observations are used to find the best combination of pre-computed unit sources which are then used as boundary conditions for real-time inundation modelling (Tang et al. 2009). The advantage of this technique is that there is increased confidence in the accuracy of the deep-water boundary conditions compared to the first approach. However, it does rely on the availability of tsunameter or other observations, which would delay the production of a forecast compared with the first approach, and in some cases, deep-water observations may be limited or even unavailable.

A third approach is to run both the deep-water forecast and the inundation model dynamically and use the real-time tsunameter observations to select one or more sets of boundary conditions, as in the previous approach. Once an earthquake occurs, a range of deep-water tsunami forecasts could be initialised and run, encompassing the range of uncertainty in the earthquake rupture details. As further seismic information and/or tsunameter observations are received in real time, some of these deep-water forecasts could be scaled or eliminated to reduce the range of uncertainty. Once complete the deep-water forecasts then provide one or more sets of boundary conditions for the inundation model. This approach would provide the best estimate for the deep-water boundary conditions, and also has the advantage of considering the uncertainty relating to the earthquake rupture. Furthermore, it could potentially provide more sophisticated forecast products, such as probabilistic information or a 'worst case' inundation forecast.

A final approach considered here could be to develop a scenario database of inundation forecasts at a site. This is similar to a system proposed by Gusman et al. (2014). For any site, an inundation model could be pre-computed for all possible earthquakes that are likely to generate a tsunami that has an impact at that location, using T2 scenarios as boundary conditions. An aspect of this method that is particularly desirable for forecasters and emergency managers is that inundation forecasts would be available almost instantaneously once the earthquake details are known, as it is a straightforward matter to select the relevant T2 scenario(s) and, hence, the relevant inundation forecast. However, there are drawbacks and limitations to this method. First, the development of this system would require considerable resources (human, computational and data storage) to pre-compute all possible inundation scenarios for even just one site, let alone multiple sites. Second, the initial conditions of the pre-computed scenarios may not exactly match the earthquake, as assumptions must be made about the details of the earthquake rupture for a pre-computed scenario. (This limitation applies also to the existing JATWC system.) Third, the system is not 'future-proofed'. For example, if there are major changes to the topography and/or bathymetry of the coastal site, such as new coastal infrastructure, harbour dredging, etc., the entire set of inundation scenarios for that site may need to be recomputed.

For this pilot study, we use approach 2, as the T2 scenarios are readily available. Approach 3 is also appealing, but it should be noted that the development work relating to use of tsunameter observations and real-time deep-water forecasts has not yet been undertaken. However, it should be a straightforward matter to substitute dynamically produced boundary conditions for T2 boundary conditions once this development work has been done.

3. Method

As this is a pilot study, just one site is considered. The location selected is Port Kembla, one of the largest industrial ports in Australia. It is located approximately 8 km south of the city of Wollongong on the New South Wales (NSW) coast, south of Sydney (see Fig. 1).

Port Kembla is a major export site for coal mined in the region. There are also a large steel works and terminals for copper, grain and automobiles. The port consists of two artificial harbours. The Outer Harbour was constructed during the first decade of the twentieth century, when two breakwaters were built. Increases in shipping traffic saw the commissioning of the construction of the Inner Harbour, with its opening in 1960 (Catterall 1994).

This site was selected for this study as it was one of five sites identified as most 'at risk' in a recent

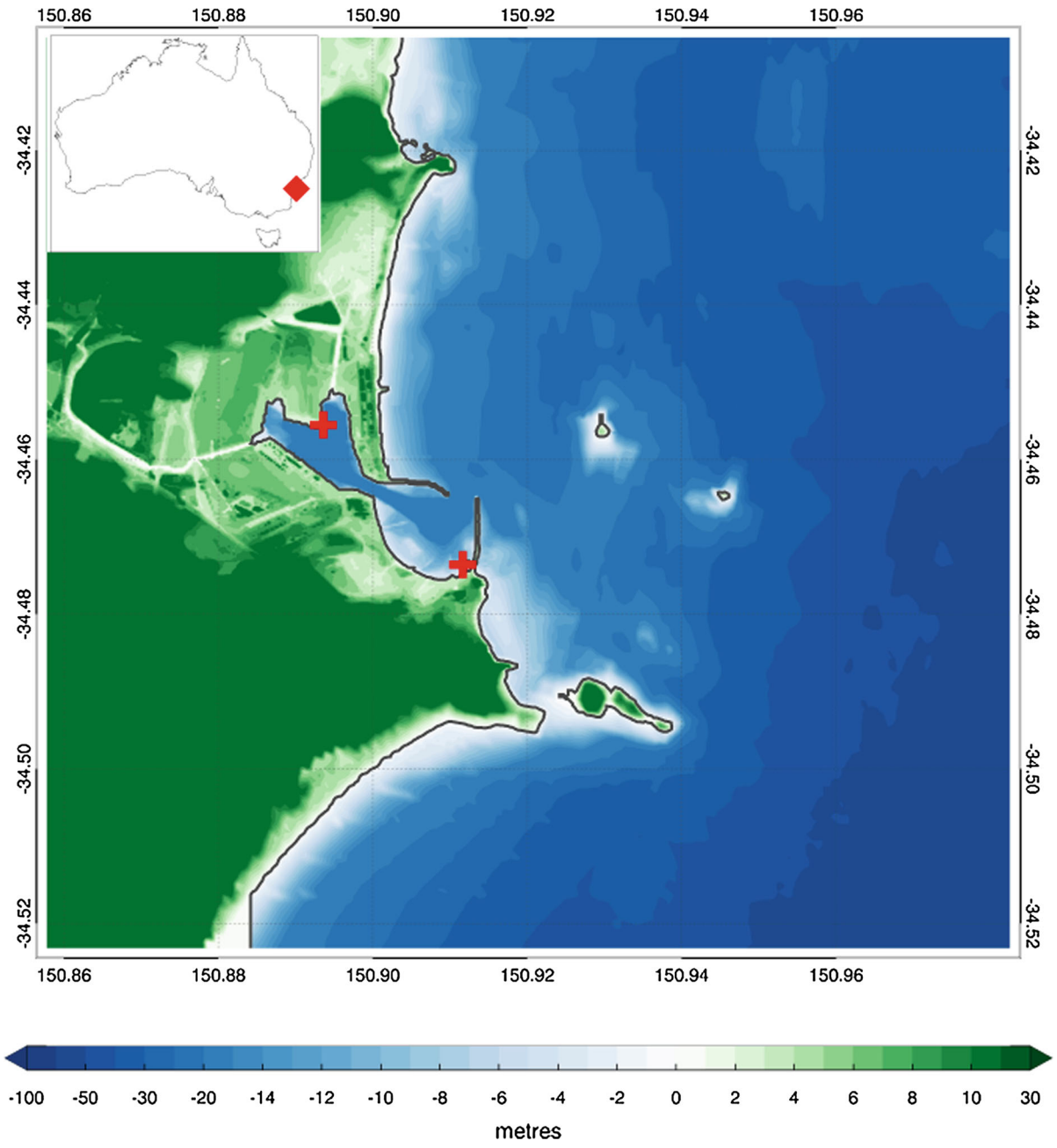

Figure 1
Map of the bathymetry of the Port Kembla region contained by the C-grid (see Sect. 3.1). The *blue shades* indicate the depth of the ocean floor below AHD and the *green shades* indicate topographic height above AHD. The *red crosses* indicate the locations of the two tide gauges. The *red diamond* on the *top-left inset figure* shows the general location of Port Kembla on the Australian coast

tsunami hazard assessment study of the NSW coastline (NSW State Emergency Service and Office of Environment and Heritage 2012) and the Digital Elevation Model (DEM) was available from that study. In addition, there are the long-term high-quality observations of sea level available from two tide gauges located within the port, and the behaviour of tsunamis at this site has been previously investigated (Hinwood and Mclean 2012). Figure 1 shows the high-resolution DEM (30-m spatial resolution)

used for the inundation modelling, and also indicates the location of the tide gauges. The zero reference level for the DEM is the Australian Height Datum (AHD), which is broadly equivalent to, in oceanographic terms, mean sea level.

From Fig. 1, it can be seen that the depth in both the Inner and Outer Harbours is relatively uniform and between 16 and 18 m. There are some areas that are shallower, particularly on the southern edge of the Outer Harbour. The port entrance into the Outer Harbour faces northwards, and the area offshore is relatively uncomplicated, with three offshore islands to the east, and natural channels to the north and east of the entrance. There is a headland to the south of the harbour, and long beaches beyond to the north and south.

The continental shelf in this part of Australia is relatively narrow and steep, with the ocean floor rising from approximately 4800 m below mean sea level at 100 km offshore, to 500 m at 35 km offshore. This has implications not only for tsunami behaviour, but also for modelling aspects.

Nine recent tsunami events (and one hypothetical event) have been used for testing, selected on the basis that they were significant enough to cause observable sea level fluctuations at the Port Kembla tide gauge sites. These events are listed in Table 1. Not surprisingly, they are almost all in the Pacific Ocean, with just one event (Sumatra 2004) in the Indian Ocean.

Following approach 2 described above, for each of these events, the 'best' T2 scenario was selected. The selected scenarios are listed in Table 1. The scenario number refers to its geographical location, and the letter refers to its moment magnitude, with $a = M_W7.5$, $b = M_W8.0$, $c = M_W8.5$, and $d = M_W9.0$. Details of the earthquake sources for the T2 scenarios can be found in Greenslade et al. (2009). The deep-water scenarios were scaled according to tsunameter observations of sea level, or to earthquake magnitude, where tsunameter observations were not available. For the first two events, tsunameter observations were not available so the scenarios were scaled according to standard operating procedures (see Greenslade et al. 2009). For the remaining events, the scenarios were scaled according to comparisons with tsunameter observations. The WMO numbers of the tsunameters used for each event are listed in Table 1.

In general, after scaling, the deep-water propagation models match the tsunameter observations very well. An example of this is shown in Fig. 2 for the Honshu 2011 event. This particular scenario and associated scaling was selected as the best option after examination of a number of different T2 scenarios and a range of scaling factors. It can be seen that the peak amplitudes are generally very well replicated. In addition, the arrival times of the largest wave are very good at tsunameters 52402 and 21413, but at the remaining three tsunameters, the modelled wave arrives too early. Examination of the locations of these tsunameters reveals that 52402 and 21413 are located to the south of the rupture, while the other three are located to the north of the rupture. The early

Table 1

List of tsunami events used for validation

Name	Date and Time	Lat	Lon	Magnitude	T2 scenario	Scaling factor	Tsunameters used for scaling
Sumatra 2004	26/12/2004 00:59	3°18′N	95°47′E	9.1	28d	1.41	N/A
Solomons 2007	01/04/2007 20:40	8°29′S	156°59′E	8.1	172b	1.41	N/A
Puysegur 2007	30/09/2007 05:23	49°23′S	134°01′E	7.4	214a	0.99	55401
Puysegur 2009	15/07/2009 09:22	45°58′S	166°28′E	7.8	218a	1.21	55013, 55015
Samoa 2009	29/09/2009 17:48	15°34′S	172°4′W	8.1	251b	1.54	51425, 51426, 54401
Chile 2010	27/02/2010 06:34	35°51′S	72°43′W	8.8	408c	2.82	32412, 32411, 51406, 43412
Honshu 2011	11/03/2011 05:46	38°19′N	142°22′E	9.0	311c	5.62	21413, 21419, 21415, 21414, 52402
Solomons 2013	06/02/2013 01:12	11°13′S	164°44″E	7.9	183b	1.60	52406, 55012, 55023
Chile 2014	01/04/2014	19°38′S	70°49′W	8.2	425b	1.32	32401, 32402, 32412
Puysegur (hypothetical)	N/A	47°38′S	166°90′E	9.0	216d	1.00	N/A

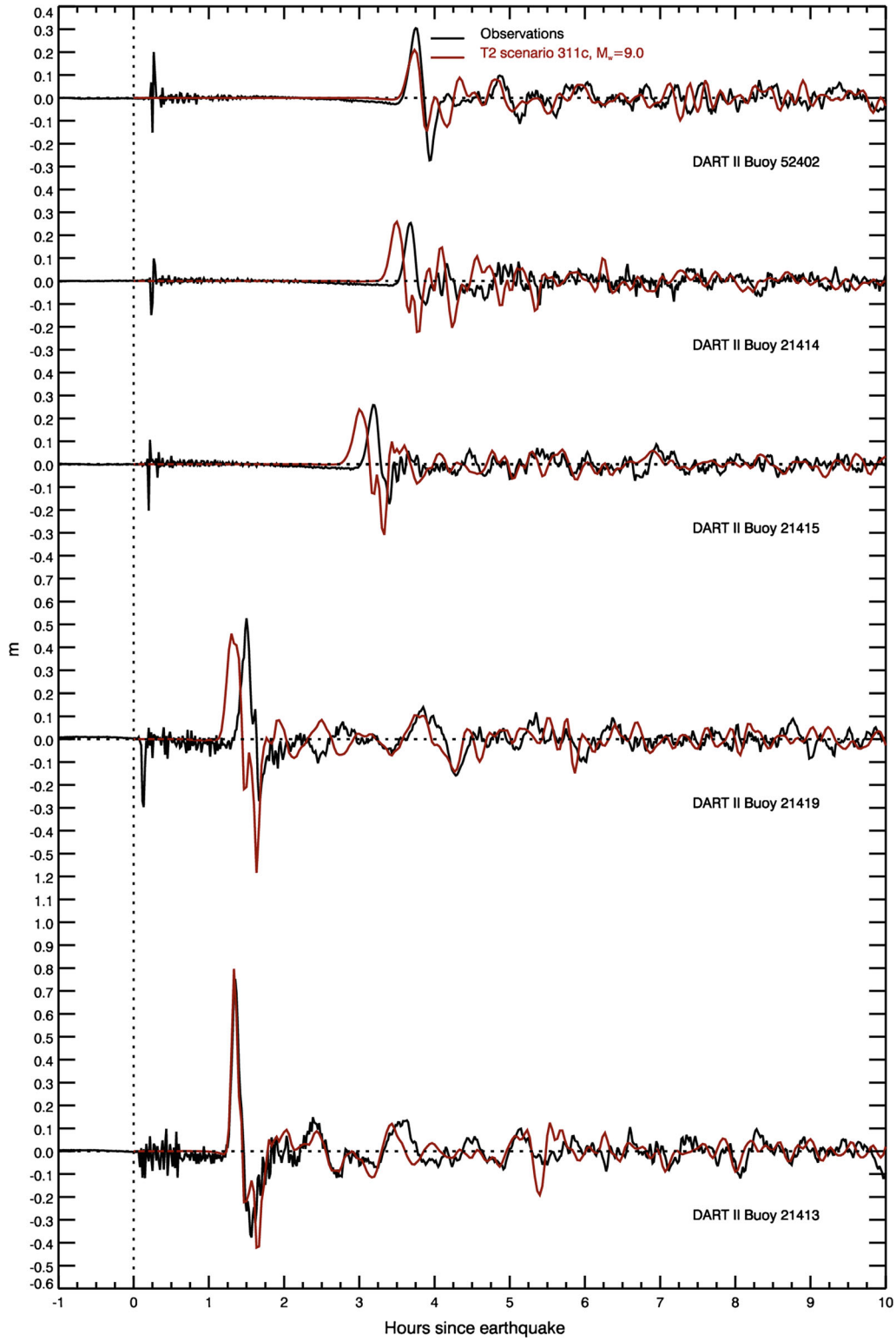

Figure 2
Scaled T2 scenario for Honshu 2011 compared to tsunameter observations

arrivals can thus be explained by the fact that the selected T2 rupture for this scenario is too long and extends too far to the north of the actual rupture. Despite this excessive rupture length, this scenario and scaling still provides the best representation of the observed signal overall, and in particular, to the south of the rupture, which is an important factor in the selection of the optimal T2 scenario for the purposes of modelling inundation at the Australian coastline. Comparisons of the deep-water scenarios with tsunameter observations were similar for the other events studied here.

Some of the scenarios needed to be rerun, as the 24-h timespan of the T2 scenario was not sufficient to capture all the sea level variability expected for the boundary conditions, particularly for distant events that may incorporate reflection or scattering from topographic features in the Pacific Ocean (Mofjeld et al. 2001). This would need to be borne in mind for potential operational implementation and is perhaps another reason to consider the third approach described above, rather than the second for future development work.

3.1. Model Details

The method of splitting tsunami (MOST) model (Titov and Synolakis 1998; Titov et al. 2016) is used for the inundation modelling. The propagation module of this model was used for developing the T2 scenarios, so nesting the models is straightforward.

The inundation model consists of three telescoping nested grids. Details of these grids are shown in Table 2. The outermost grid, hereafter referred to as the 'A-grid', is the most coarse of the grids and is forced at its boundaries by the (scaled) archived T2 scenarios. These T2 boundary conditions are provided at 4 arc minute spatial intervals and 2-min temporal intervals (Greenslade et al. 2009). As stated above, some of these scenarios have been rerun for a longer period, so that there is at least 48 h of boundary forcing available from the time of the earthquake.

The A-grid, in turn, provides boundary forcing for the intermediate grid, hereafter known as the 'B-grid' which in turn provides boundary forcing for the finest grid, hereafter referred to as the 'C-grid'. Given the grid specifications in Table 2, the model was run with a time step of 0.75 s, with the B-grid calculated at every time step and the A-grid calculated every fourth time step. The model does not begin computations until a disturbance of 1 mm is measured in the boundary conditions of the A-grid. All grids are set to be capable of inundating, that is, an algorithm that calculates the wetting and drying of cells is applied to all three grids. The Manning's coefficient of friction is uniform over the grids and set to 9×10^{-4} s/m$^{1/3}$.

To confirm the stability of the inundation model, a hypothetical large event (a $M_w = 9.0$ occurring on the Puysegur trench, see Table 1) was simulated. This ran to completion providing a certain level of confidence in the robustness of the model. The resulting inundation is shown in Fig. 3. It can be seen that significant portions of the coast both outside and inside the harbours are predicted to experience inundation from this hypothetical event.

3.2. Observations

Apart from the hypothetical event described above, none of the actual events listed in Table 1 were significant enough to cause any observed inundation, so validation and verification are necessarily limited to the tide gauge observations of sea level. As noted previously, observations of sea level from two tide gauges within the harbour were

Table 2

Specifications for the inundation grids

Grid	Resolution (Arc s)	Resolution (m)	Dimensions	Physical size (km)	Maximum depth (m)	Maximum time step (s)
A	30	900	249 × 280	190 × 260	4959	3.4
B	10	300	350 × 389	90 × 120	4789	1.15
C	1	30	450 × 425	11 × 13	75	0.94

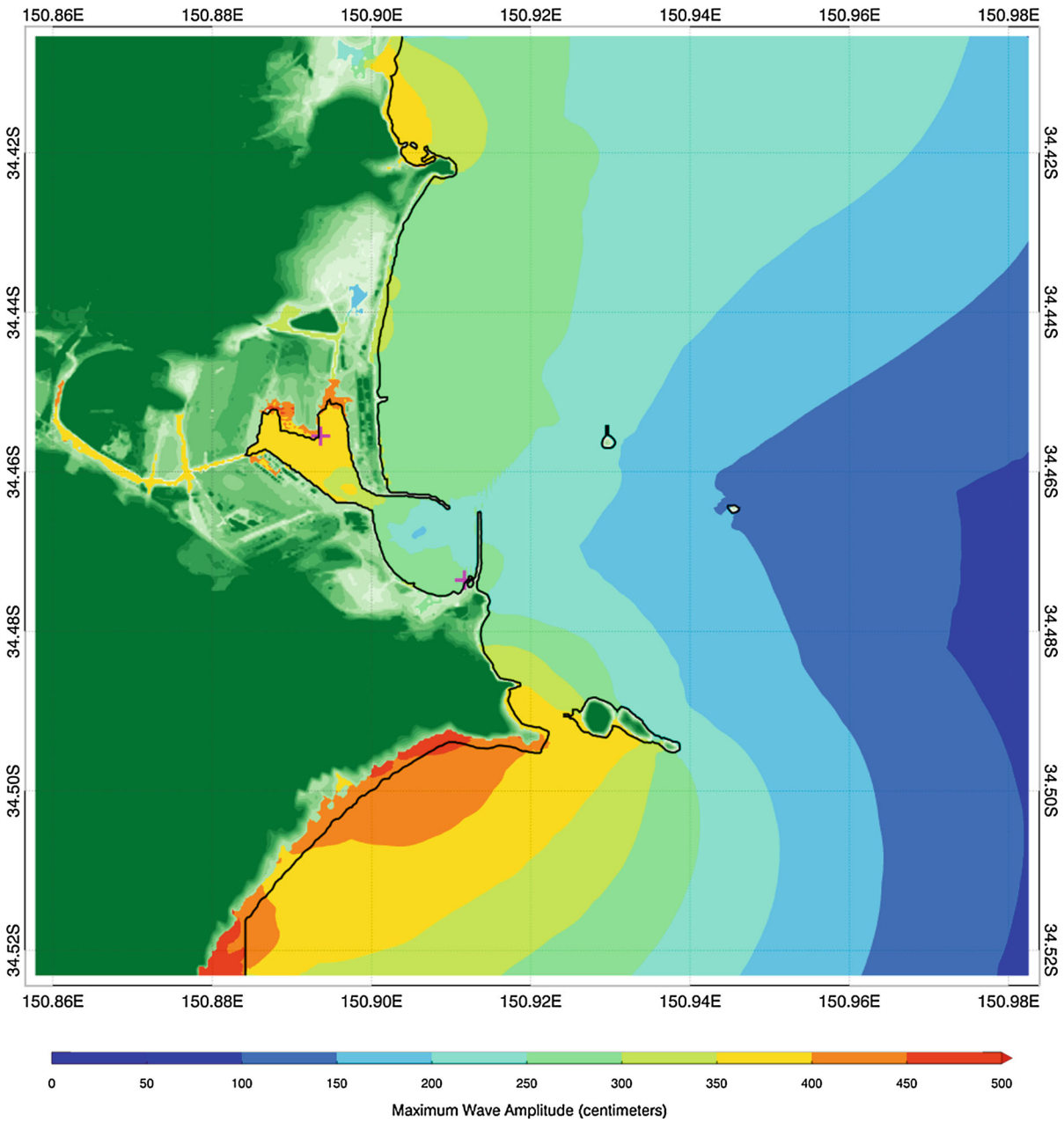

Figure 3
Inundation extent for the hypothetical Mw = 9.0 event on the Puysegur trench, represented as maximum wave amplitude above AHD

available. Their locations are indicated in Fig. 1. The gauge located in the Outer Harbour provided data at 1-min intervals; however, the Inner Harbour tide gauge data were available only at 10-min intervals, which mean that the variability is likely to be undersampled at this gauge. In addition, there were no data available from the Inner Harbour gauge for two events studied here, Sumatra 2004 and Samoa 2009. Furthermore, the gauge is not ideally located for observing tsunamis, being on the internal (coastal) side of a large jetty-type structure that runs parallel to the shore. These are significant limitations that suggest care must be taken when interpreting the results at this tide gauge.

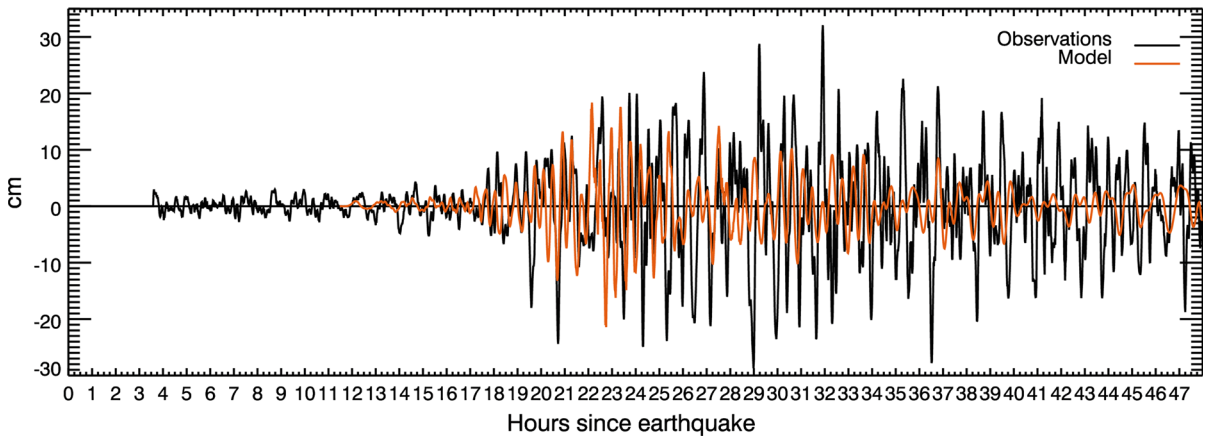

Figure 4
Time series of modelled and observed sea level for Sumatra 2004 at the Outer Harbour tide gauge. Since observations from the Inner Harbour tide gauge were not available for this event, results are not shown for that location

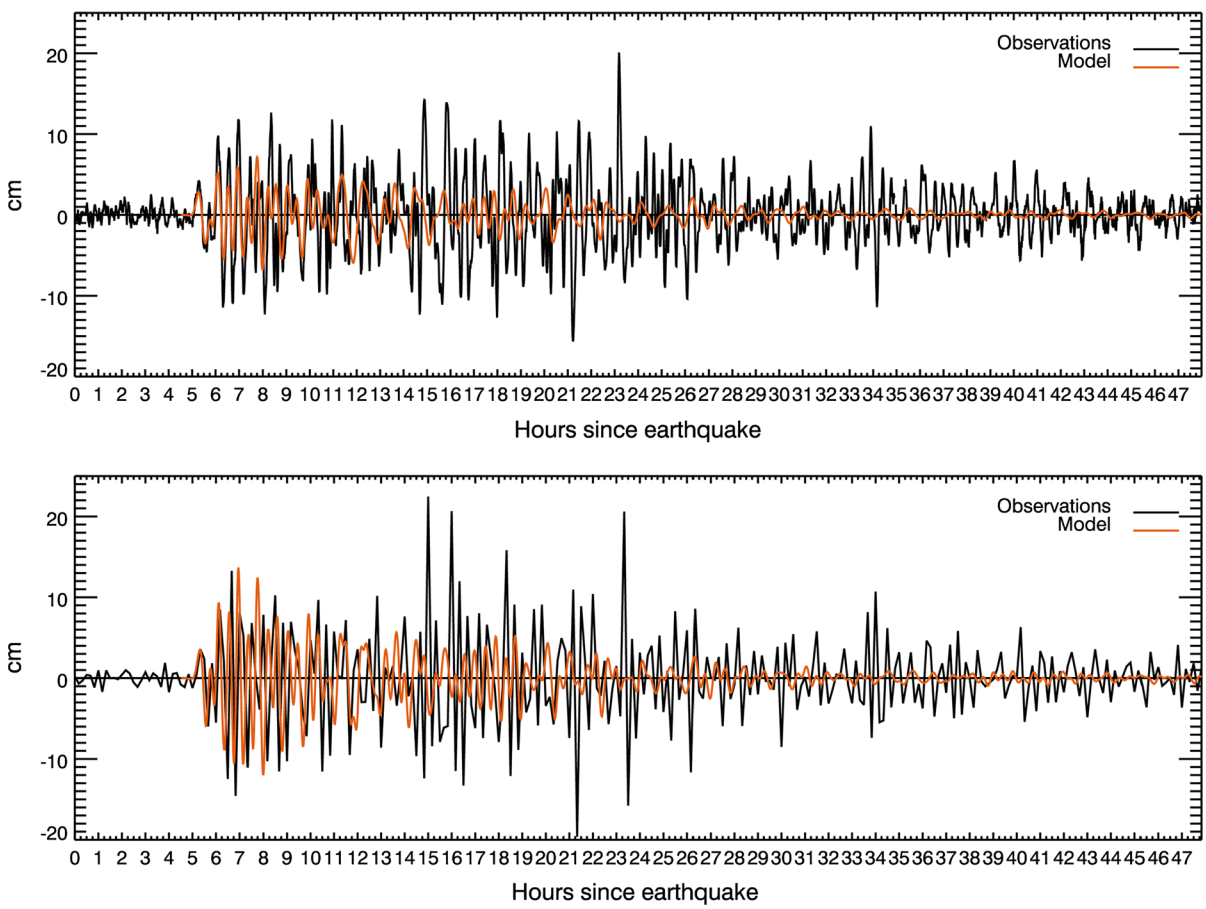

Figure 5
Time series of modelled and observed sea level for Solomons 2007 at the Outer Harbour tide gauge (*top panel*) and the Inner Harbour tide gauge (*bottom panel*)

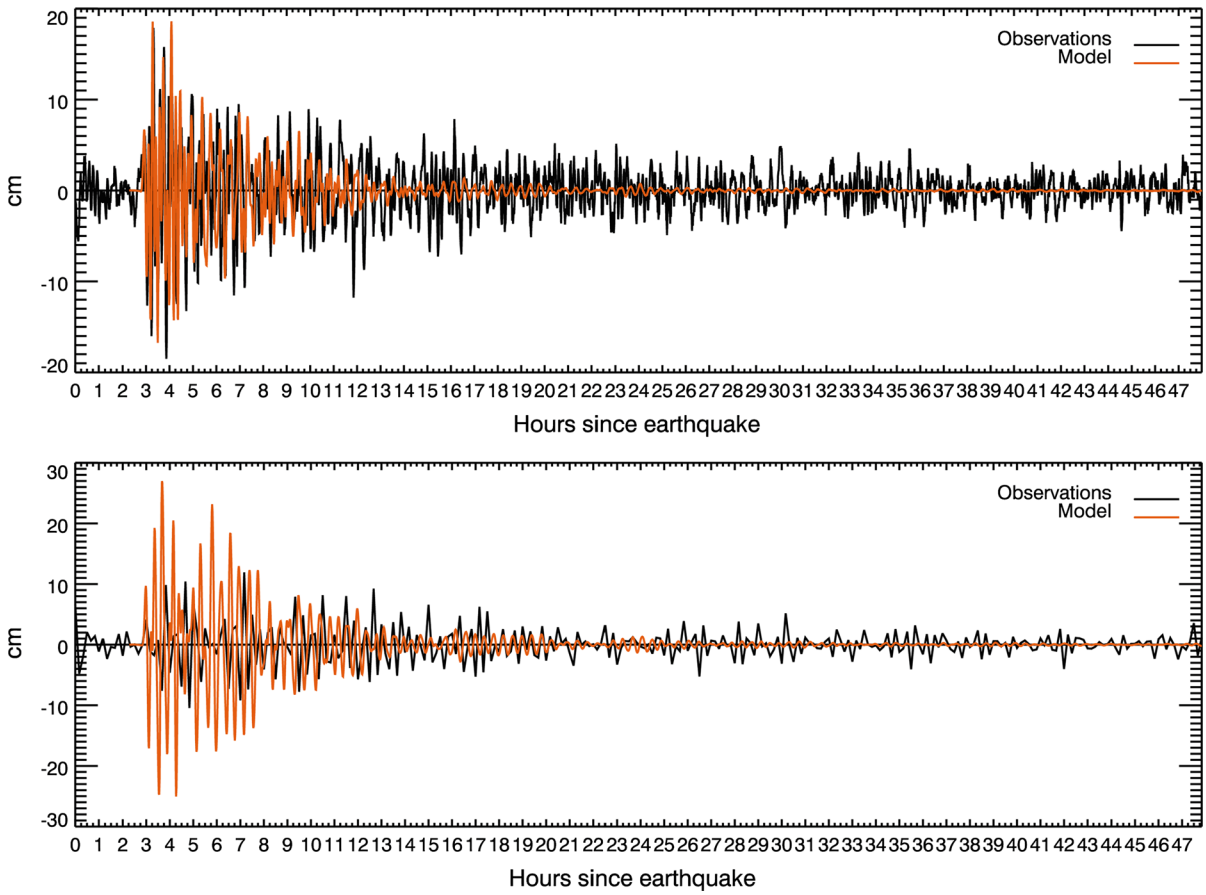

Figure 6
Time series of modelled and observed sea level for Puysegur 2007 at the Outer Harbour tide gauge (*top panel*) and the Inner Harbour tide gauge (*bottom panel*)

To be able to compare these observations to the model output, the tsunami signal needs to be isolated as much as possible from the total sea level signal. Astronomical tides are generally the main contributor to sea level variability recorded by coastal tide gauges, but there are many other sources of variability present. Isolation of the tsunami signal was undertaken by applying a high-pass filter to remove the low-frequency components of the observed sea level such as tides. The filter is a Kaiser–Bessel filter, with a cut-off period of 180 min and 300 weights for the 1-min Outer Harbour gauge and 100 weights for the 10-min Inner Harbour gauge. In general, this filtering performs well in terms of isolating the tsunami signal, but in most cases, there is some existing sea level variability at similar frequencies to the tsunami signal which is visible as oscillations before the tsunami arrives at the tide gauge. It is not possible to remove this non-tsunami variability using this filtering technique.

4. Results

Comparisons of observed and modelled sea level (from the C-grid) for each event, at the Outer Harbour and Inner Harbour tide gauges (where available), are shown in Figs. 4, 5, 6, 7, 8, 9, 10, 11, and 12. In general, it can be seen that the model captures the key features of each event very well. In particular, the tsunami arrival times are very well depicted, and also the overall envelope of the variability over time is captured very

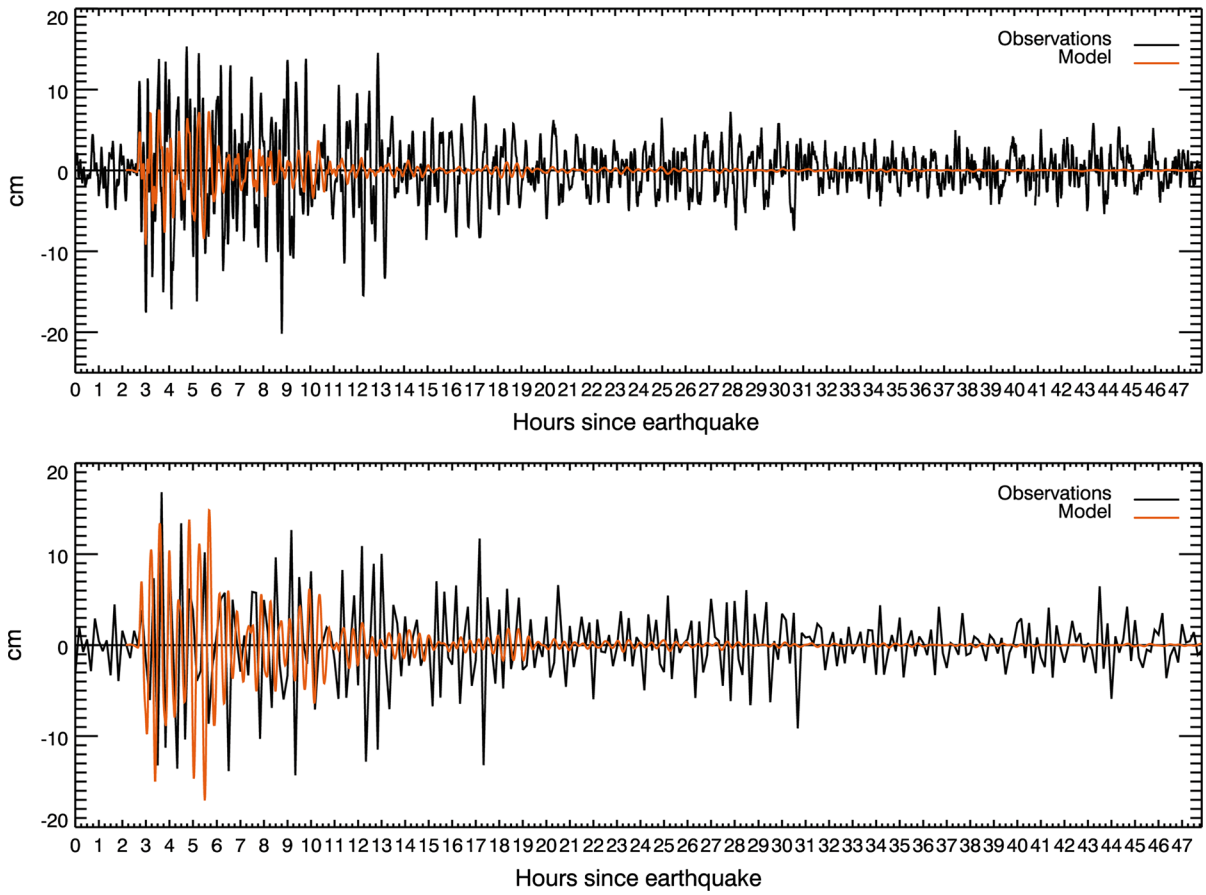

Figure 7
Time series of modelled and observed sea level for Puysegur 2009 at the Outer Harbour tide gauge (*top panel*) and the Inner Harbour tide gauge (*bottom panel*)

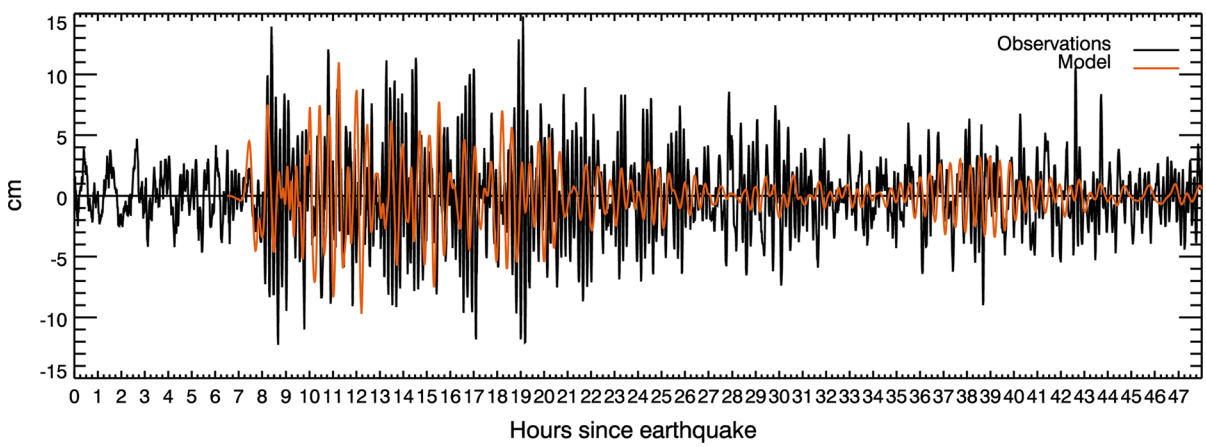

Figure 8
Time series of modelled and observed sea level for Samoa 2009 at the Outer Harbour. Since observations from the Inner Harbour tide gauge were not available for this event, results are not shown for that location

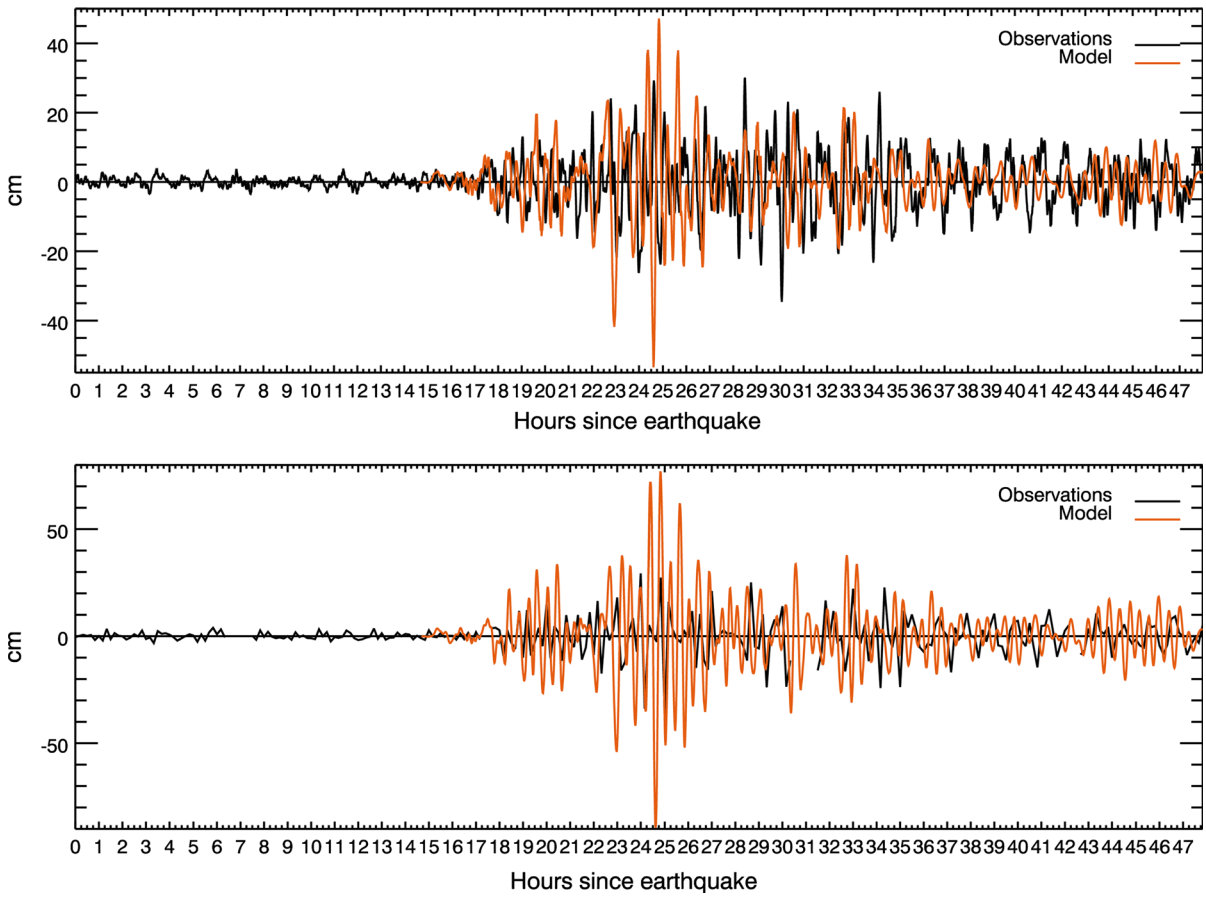

Figure 9
Time series of modelled and observed sea level for Chile 2010 at the Outer Harbour tide gauge (*top panel*) and the Inner Harbour tide gauge (*bottom panel*)

well by the model. However, recall that little weight should be placed on the comparisons at the Inner Harbour due to the limitations of the observations there.

The key warning parameter of interest, in addition to arrival time, is maximum (positive) amplitude. It can be seen that for some events, the peak amplitude is well captured, but in others, it is over- or underestimated. Table 3 lists the differences in maximum (positive) amplitude, both as raw difference and as a percentage of the observed value for all events considered here. At the Inner Harbour gauge, it can be seen that in 4 out of 7 cases, the model significantly overestimates the maximum amplitude—this is likely related to the coarse temporal frequency of the observations. At the Outer Harbour, the modelled maximum (positive) amplitude is on average 8 cm (i.e. 36 %) away from the observed value, however, this is neither consistently overpredicted, or consistently underpredicted, as the mean bias over all events is −1 cm, i.e. an average underestimation of 1 cm (2 %).

5. *Discussion*

There are some interesting features of a few of the events studied. There are discussed here in more detail.

For Sumatra 2004 (Fig. 4), the timing of the maximum amplitude occurs much earlier in the model (around 22 h after the earthquake) than in the observations (around 32 h after the earthquake. This

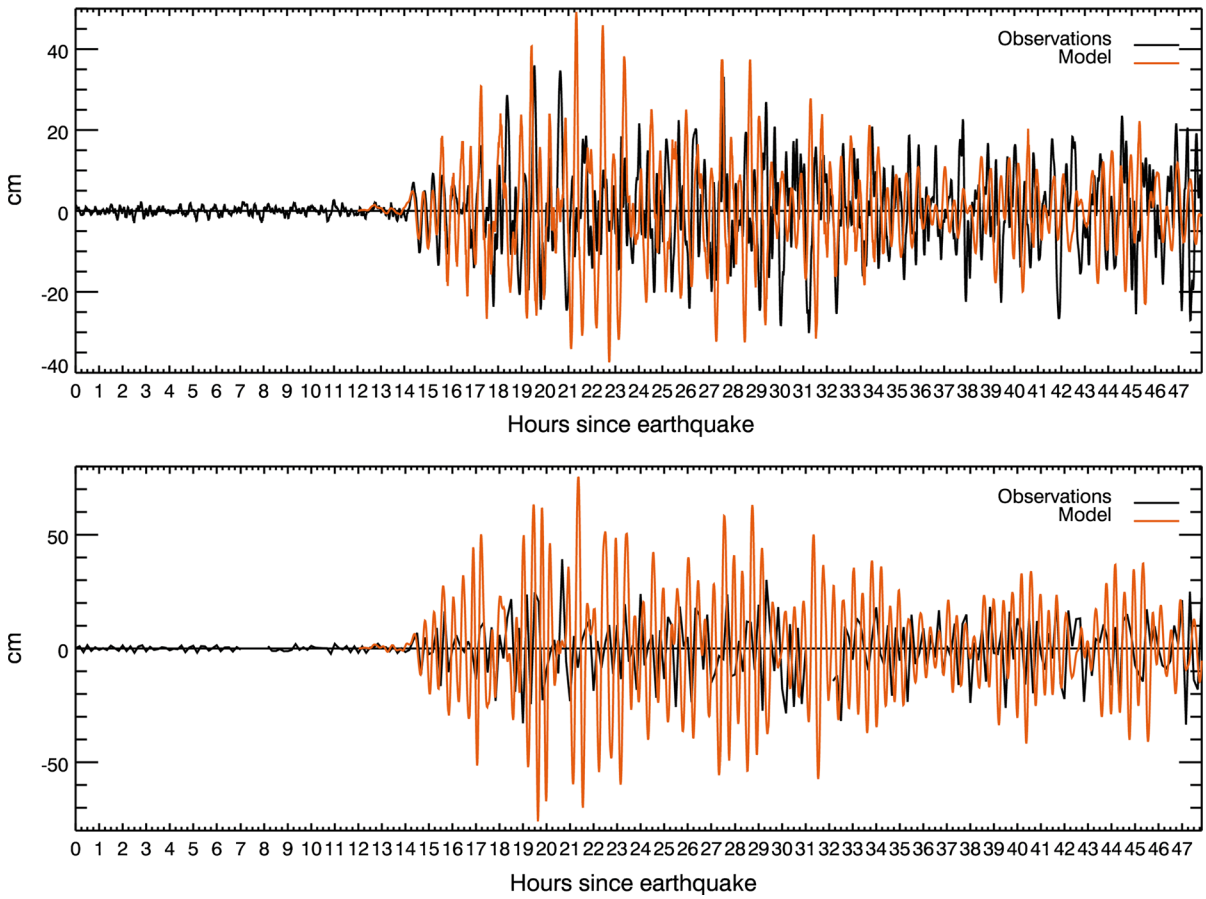

Figure 10
Time series of modelled and observed sea level for Honshu 2011 at the Outer Harbour tide gauge (*top panel*) and the Inner Harbour tide gauge (*bottom panel*)

large difference in the timing of the maximum amplitude may be due, in this case, to the limited model domain used for the deep-water propagation runs. The longitudinal extent of the T2 domain is from 30°E to 300°E, so the only possible propagation path for the modelled tsunami is in an easterly direction to the south of Australia. There is an alternate path to the west, around Africa, South America and across the Pacific, and there has been some suggestion that the tsunami signal could be expected to be seen on the east coast of Australia along this propagation path (Titov et al. 2005). This path is considerably longer, and so arrival times would be expected to be much later. Given that this propagation path does not exist in in the deep-water simulations used here, this could provide an explanation for the lack of the delayed higher waves in the modelled simulation. Another explanation could be that the sea level within the harbour continues to oscillate and amplify through natural seiching, reflections etc., and this is not completely captured by the model.

Samoa 2009 (Fig. 8) is characterised by higher frequency variability than most other events, which can be seen in the observed sea level before the arrival of the tsunami about 8 h after the earthquake. Another interesting feature of this event is the increased variability that can be seen in the modelled time series approximately 35–40 h after the event. This is less obvious in the observations, but there do

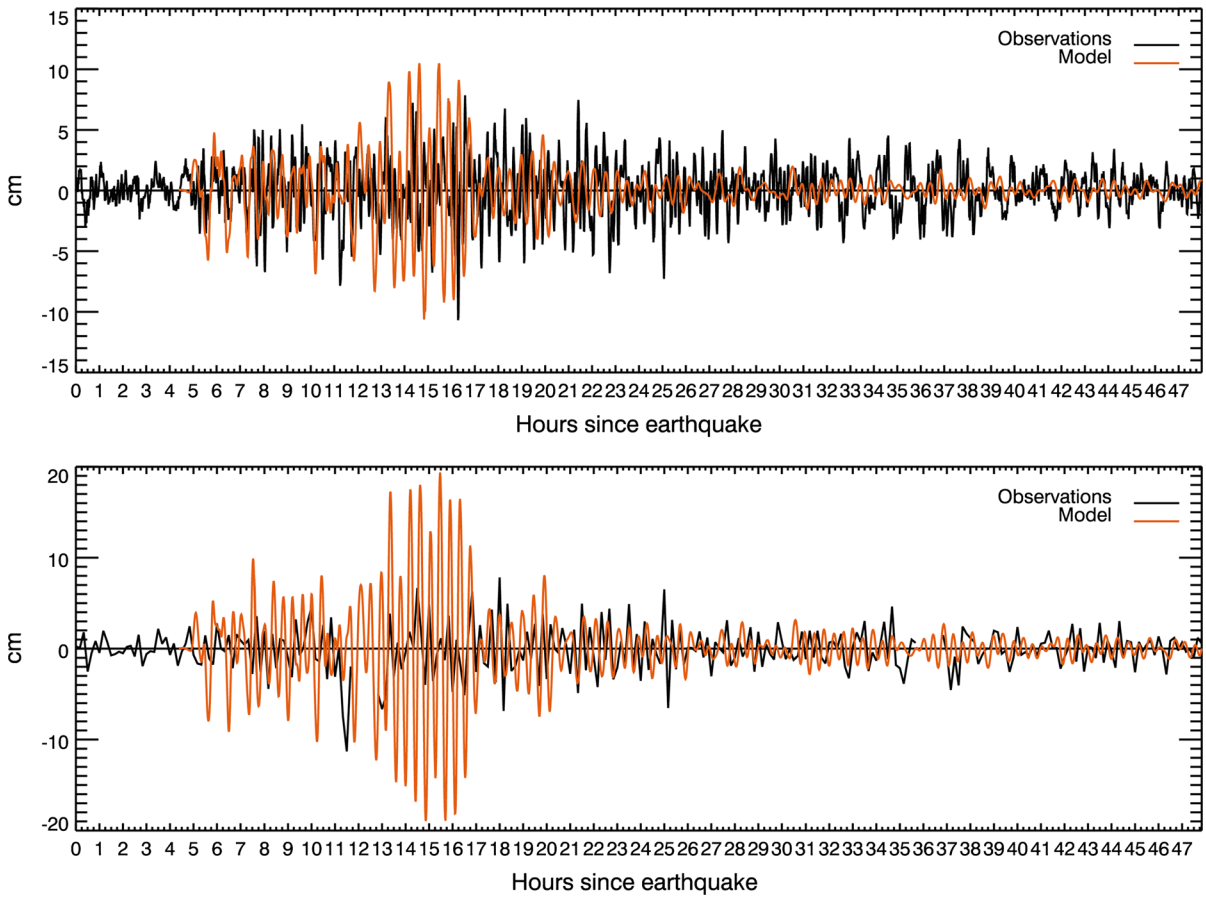

Figure 11
Time series of modelled and observed sea level for Solomons 2013 at the Outer Harbour tide gauge (*top panel*) and the Inner Harbour tide gauge (*bottom panel*)

appear to be some observed waves occurring very late. Inspection of the animated propagation model simulation suggests that this is likely to be due to the arrival of waves reflected from the eastern land boundary of the Pacific Ocean.

An interesting note relating to the last two events, Solomons 2013 and Chile 2014, is that there was some significant construction activity undertaken in the Outer Harbour in 2012. Satellite imagery of the port before and after this construction is shown in Fig. 13. Changes to areas above the sea level can be identified in the imagery, such as the new structure formed on reclaimed land; however, changes below the sea surface, such as those due to dredging are not able to be identified. The DEM used for all events studied here was developed prior to this construction and, therefore, did not include these changes. It could be expected that the changed DEM may results in different modelled time series. This could be tested by creating a new DEM reflecting the new construction and rerunning the model. This is not done here, but left for future work.

6. Outlook

The results of the previous sections have demonstrated that the quality of inundation forecasting is likely good enough to be able to be used operationally in a tsunami warning system. At the

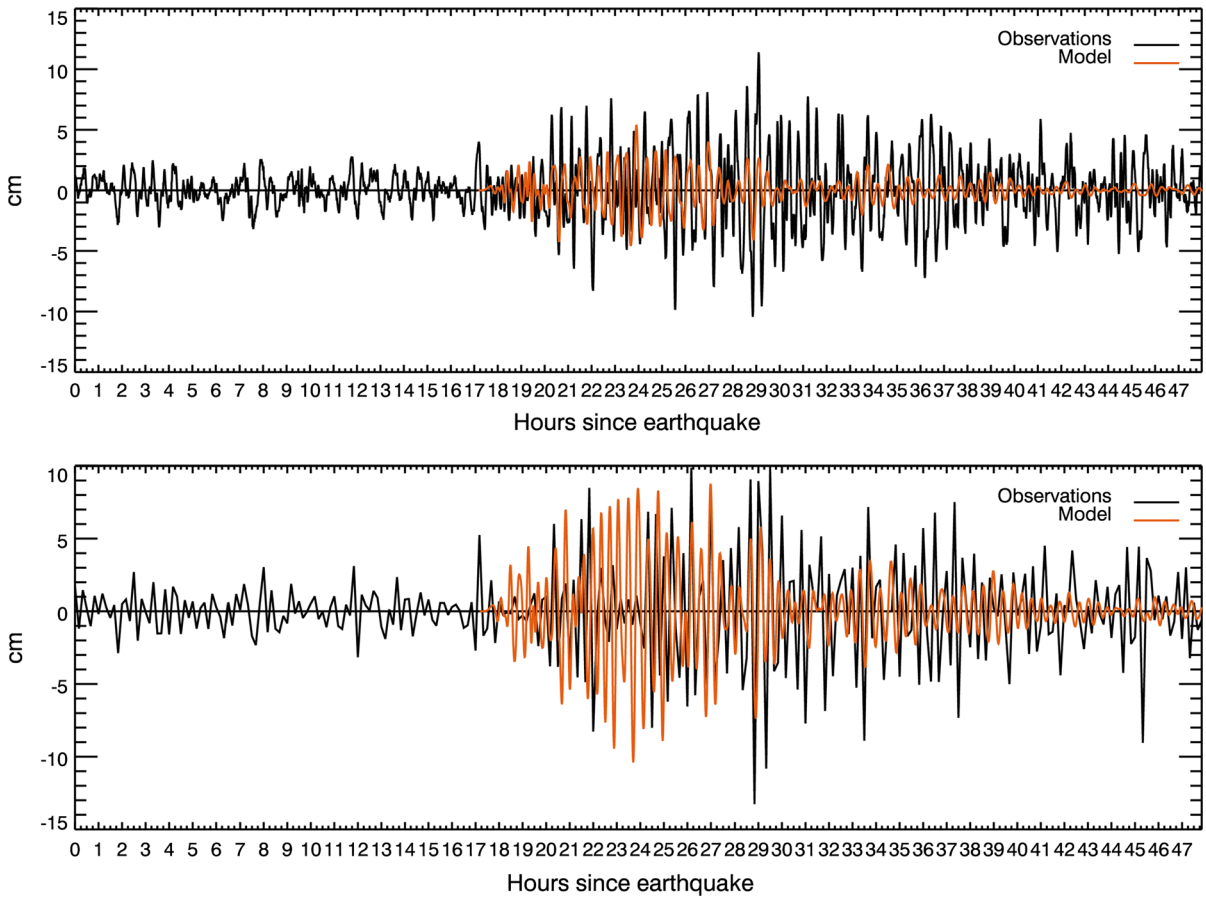

Figure 12
Time series of modelled and observed sea level for Chile 2014 at the Outer Harbour tide gauge (*top panel*) and the Inner Harbour tide gauge (*bottom panel*)

very least, the results show that there are no persistent biases in the forecasts that would need to be addressed. A further issue that is worth considering is whether the development of an operational inundation forecasting system is feasible, given the Australian context.

To establish an inundation forecast system, a prerequisite is the availability of high-resolution DEMs. These are starting to become available, but they need regular assessment and updating, as shown in Fig. 13.

A further consideration is the computational resources needed to provide timely forecasts. Australia has the luxury of having no subduction zones that are closer than approximately 2-h tsunami travel time away with the Puysegur trench south of New Zealand being the 'closest' potential source zone. The aim of the JATWC is to be able to issue warnings at least 1.5 h prior to possible impact for the Australian mainland. This allows, in the most extreme case, only 30 min for assessing potential impacts after an earthquake, including the time taken for seismic analysis. The initial estimated computational run time for a full 24-h inundation forecast is around 45 min on the Bureau of Meteorology's current computing infrastructure. Given the current warning requirements, this is too slow for tsunamis generated by earthquakes on the Puysegur trench, but would be adequate for tsunamis generated elsewhere. However, it is likely that the computational run time would be reduced considerably with planned upgrades to the Bureau of Meteorology's supercomputer and with effort put into optimizing the inundation model.

Table 3

Observed and modelled maximum value for each event

	Obs max (cm)	Model max (cm)	Model-Obs (cm)	100 × (Model-Obs)/Obs (%)	abs(Model-Obs) (cm)	100 × abs(Model-Obs)/Obs (%)
Outer Harbour						
Sumatra 2004	32	18	−14	−43	14	43
Solomons 2007	20	7	−13	−64	13	64
Puysegur 2007	18	19	1	4	1	4
Puysegur 2009	15	8	−8	−51	8	51
Samoa 2009	15	11	−4	−26	4	26
Chile 2010	30	47	17	57	17	57
Honshu 2011	36	49	13	37	13	37
Solomons 2013	8	10	3	34	3	34
Chile 2014	10	9	−1	−11	1	11
Average			−1	−2	8	36
Inner Harbour						
Solomons 2007	22	14	−9	−39	9	39
Puysegur 2007	12	27	15	126	15	126
Puysegur 2009	17	15	−2	−12	2	12
Chile 2010	29	77	48	162	48	162
Honshu 2011	39	75	36	91	36	91
Solomons 2013	8	19	11	144	11	144
Chile 2014	11	5	−6	−53	6	53
Average			13	76	20	90

Note that the calculations were performed on more precise data (two decimal places) before rounding

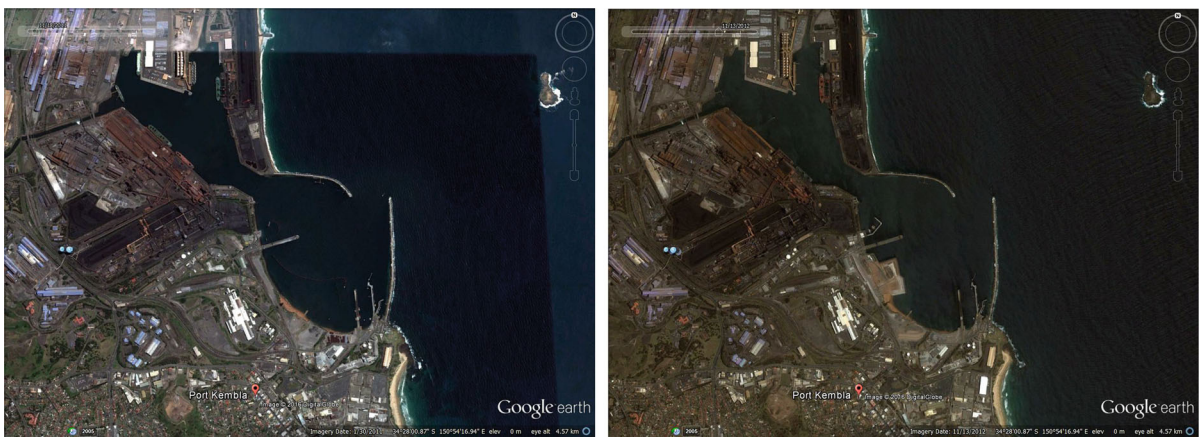

Figure 13
Google earth imagery showing the construction in the Outer Harbour that was undertaken between November 18, 2011 (*left panel*) and November 13, 2012 (*right panel*) (Images: Google, DigitalGlobe)

Indeed, Oishi et al. (2015) demonstrated that they have the ability to run an inundation model 75 times faster than real time, indicating that there is potential for a feasible solution.

A final note is in relation to stakeholder engagement. It is vitally important to engage with the potential users of these possible products, i.e. emergency management organisations at an early stage. These have a number of benefits—first, it ensures that the forecasts and products that are being produced are actually what they want and can use, and second, when stakeholders have an input into development of new products, this will ensure stronger uptake and use of the products by them.

Acknowledgments

The authors would like to acknowledge the Port Authority of NSW for providing sea level data from Port Kembla Inner Harbour tide gauge. We would also like to thank Mr. Chris Moore, and the NOAA Centre for Tsunami Research for providing the software used for propagation and inundation modelling. Dr. Robert Greenwood, Dr. Eric Schulz and three external reviewers provided useful comments that improved the manuscript.

References

Allen, S. C. R., & Greenslade, D. J. M. (2010). Model-based tsunami warnings derived from observed impacts. *Natural Hazards and Earth Systems Sciences, 10*(2631–2642), 2010. doi:10.5194/nhess-10-2631-2010.

Bernard, E., & Titov, V. (2015). Evolution of tsunami warning systems and products. *Philosophical Transactions of the Royal Society A, 373*(2053), 20140371. doi:10.1098/rsta.2014.0371.

Borrero, J. C., Sieh, K., Chlieh, M., & Synolakis, C. E. (2006). Tsunami inundation modelling for western Sumatra. *Proceedings of the National Academy of Sciences of the United States of America, 103*, 19673.

Catterall, C., Catterall, K., Claussen, W., Claussen, D., King, B., King, M., McNamara, D., Parsons, J., Parsons, M., Simons, M. & Treble, R. (1994). A Living History of Port Kembla. The Living History Team.

Gonzalez, F. I., Titov, V. V., Mofjeld, H. O., Venturato, A. J., Simmons, S., Hansen, R., et al. (2005). Progress in NTHMP hazard assessment. *Natural Hazards,35*, 89–110.

Greenslade, D. J. M., Allen, S. C. R., & Simanjuntak, M. A. (2010). An Evaluation of Tsunami Forecasts from the T2 Scenario Database. *Pure and Applied Geophysics, 168*(6–7), 1137–1151. doi:10.1007/s00024-010-0229-3.

Greenslade, D.J.M., Simanjuntak, M.A. & Allen, S.C.R. (2009). An enhanced tsunami scenario database: T2, CAWCR Technical Report No. 014, Melbourne: Bureau of Meteorology, 30 pp.

Grilli, S. T., O'Reilly, C., Harris, J. C., Tajalli Bakhsh, T., Tehranirad, B., Banihashemi, S., et al. (2015). Modeling of SMF tsunami hazard along the upper U. S. East Coast: Detailed impact around Ocean City, MD. *Natural Hazards, 76*, 705–746. doi:10.1007/s11069-014-1522-8.

Gusman, A. R., Tanioka, Y., MacInnes, B. T., & Tsushima, H. (2014). A methodology for near-field tsunami inundation forecasting: application to the 2011 Tohoku tsunami. *Journal of Geophysical Research: Solid Earth, 119*(11), 8186–8206.

Hinwood, J. B., & Mclean, E. J. (2012). Effects of the March 2011 Japanese tsunami in bays and estuaries of SE Australia. *Pure and Applied Geophysics, 170*(6), 1207–1227. doi:10.1007/s00024-012-0561-x.

Horspool, N., Griffin, J. & Van Putten, K. (2010). Tsunami modelling validation: the impact of the 2004 Indian Ocean Tsunami on Geraldton, Western Australia, Geoscience Australia Record 2010/01.

Løvholt, F., Kaiser, G., Glimsdal, S., Scheele, L., Harbitz, C. B. & Pedersen, G. (2012). Modeling propagation and inundation of the 11 March 2011 Tohoku tsunami. *Natural Hazards and Earth System Sciences*, *12*, 1017–1028, doi:10.5194/nhess-12-1017-2012.

Mofjeld, H. O., Titov, V. V., Gonzalez, F. I., & Newman, J. C. (2001). Tsunami scattering provinces in the Pacific Ocean. *Geophysical Research Letters V, 28*(2), 335–338.

NSW State Emergency Service and Office of Environment and Heritage (2012). Final Draft NSW Tsunami Inundation Modelling and Risk Assessment, *Cardno Technical Report* LJ2874/Rep2703, 87 pp.

Oishi, Y., Imamura, F., & Sugawara, D. (2015). Near-field tsunami inundation forecast using the parallel TUNAMI-N2 model: application to the 2011 Tohoku-Oki earthquake combined with source inversions. *Geophysical Research Letters,*. doi:10.1002/2014GL062577.

Tang, L., Titov, V. V., & Chamberlin, C. D. (2009). Development, testing, and applications of site-specific tsunami inundation models for real-time forecasting. *Journal Geophysical Research, 114*, C12025. doi:10.1029/2009JC005476.

Titov, V., Kânoğlu, U., & Synolakis, C. (2016). Development of MOST for Real-Time Tsunami Forecasting. *Journal of Waterway, Port, Coastal, and Ocean Engineering,*. doi:10.1061/(ASCE)WW.1943-5460.000035703116004.

Titov, V. V., Moore, C., Greenslade, D. J. M., Pattiaratchi, C., Badal, R., Synolakis, C. E., et al. (2011). A new tool for inundation modeling: community Modeling Interface for Tsunamis (ComMIT). *Pure and Applied Geophysics,*. doi:10.1007/s00024-011-0292-42121-2131.

Titov, V. V., Rabinovich, A. B., Mofjeld, H. O., Thomson, R. E., & González, F. I. (2005). The Global Reach of the 26 December 2004 Sumatra Tsunami. *Science, 309*(5743), 2045–2048. doi:10.1126/science.1114576.

Titov, V. V., & Synolakis, C. S. (1998). Numerical modeling of tidal wave runup. *Journal of Waterway, Port, Coastal, and Ocean Engineering, 124*(4), 157–171. doi:10.1061/(ASCE)0733-950X(1998)124:4(157).

Uslu, B., & Greenslade, D. J. M. (2013). Validation of Tsunami Warning Thresholds Using Inundation Modelling, CAWCR Technical. 062, Melbourne: Bureau of Meteorology, 17 pp.

Wei, Y., Fritz, H., Titov, V., Uslu, B., Chamberlin, C., & Kalligeris, N. (2015). Source models and near-field impact of the April 1, 2007 Solomon Islands tsunami. *Pure and Applied Geophysics,*. doi:10.1007/s00024-014-1013-6657-682.

(Received May 12, 2016, revised August 29, 2016, accepted August 31, 2016, Published online October 14, 2016)